scientific reports

OPEN

Diagenetic facies and pore evolution of tight sandstone reservoirs of the Jiamuhe formation in the Shawan sag, Junggar basin

Yao Zongquan[1,2]✉, Fu Tianyu[1,2], Wang Jun[3], Zhang Xiaohong[4], Jia Chunming[5], Wei Wang[1,2], Deleqiati Jianatayi[1,2], Yu Haitao[5], Li Jing[5] & Wang Haoyi[1,2]

The Jiamuhe Formation in the northwest margin of the Shawan Sag comprises tight sandstone reservoirs, and its distribution has obvious regional differences, but the reasons for this difference are not clear. This study aims to clarify the diagenetic facies and pore evolution patterns by integrating petrographic thin sections, fluorescence thin sections, X-ray diffraction, porosity-permeability data. The objective is to identify the causes of these differences, establish a theoretical evolutionary model, and quantitatively characterize pore evolution. The study area is dominated by lithic sandstone, feldspar lithic sandstone, and lithic feldspar sandstone. These rocks are characterized by relatively low textural and compositional maturity. The primary storage space is predominantly composed of secondary pores formed through dissolution, with minor microfractures present. The findings indicate that dissolution is the principal factor contributing to the physical properties of reservoirs observed between the delta plain and delta front. The texture of the cement and secondary pores govern the variations in physical properties within the same facies zone. The diagenetic sequence includes compaction→early chlorite coating→early meteoric water dissolution→early calcite/kaolinite cementation→middle-stage analcime/philipsite/zeolite cementation →middle-stage organic acid dissolution→microfractures. Quantitative analysis indicates that the original porosity decreased 23.89% by compaction and 7.94% by cementation. Conversely, dissolution and tectonic fracturing enhance porosity by 5.87% and 5.10%, respectively. The theoretical calculations align well with the experimental results. Based on the cementation-sedimentation-pore type, the Jiamuhe Formation in the study area is classified into four distinct diagenetic facies, type I is strong cementation – outer delta front – dissolution pores. Type II is strong cementation – inner delta front – intra granular dissolution pores with moderate dissolution. Type III is poor cementation – delta plain – intergranular pores with strong dissolution. Type IV is strong compaction – delta plain – intergranular dissolution pores with moderate cementation. The evolutionary history of each facies was reconstructed by using porosity evolution curves. Type I and Type III were demonstrated significant reservoir potential, offering a reference for predicting favorable reservoir distribution in future studies.

Keywords Diagenesis, Porosity quantification, Jiamuhe formation, Shawan Sag

Tight reservoirs have become a hotspot in unconventional oil and gas exploration due to their wide distribution and high potential of oil and gas resource[1]. In recent years, rapid development and innovation in new theories (continuous accumulation theory[2], unconventional petroleum geology[3], unconventional petroleum sedimentology[4],and technologies (nano size pore-throats) have showcased their enormous potential[5]. However, challenges such as strong diagenesis, poor reservoir properties, and high heterogeneity have become key difficulties in the exploration and development of high-quality reservoirs[6–10]. There is a spatiotemporal relationship between diagenetic facies and sedimentary facies, indicating a certain pattern in the distribution of diagenetic faices within sandbodies[2]. Eodiagenesis facies were proposed as an important approach to solve

[1]School of Geology and Mining Engineering, Xinjiang University, Urumqi 830047, China. [2]Key laboratory of Central Asian Orogenic Belts and Continental Dynamics, Urumqi 830047, China. [3]SINOPEC Geophysical Research Institute Co., Ltd, Nanjing, Jiangsu, China. [4]Zhundong Oil Production Plant, Xinjiang Oilfield, Urumqi 830047, China. [5]Research Institute of Exploration and Development, PetroChina Xinjiang Oilfield, Urumqi 830014, China. ✉email: yzq@xju.edu.cn

the diagenesis and heterogeneity in carbonate reservoirs[11]. After being introduced to China, this concept was extended to encompass a understanding of diagenetic environments and products, including petrological geochemical, and petrophysical characteristics[12]. To date, many researchers emphasized that diagenetic facies serve as physical indicators of the diagenetic environment[12,13]. However, due to varying classification criteria, there is no standardized naming convention for diagenetic facies[14]. Nevertheless, the general consensus is that the diagenetic facies, by highlighting the current characteristics and formation of reservoirs, help to summarize the regional patterns of diagenetic evolution[15–17].

Most scholars believe that the formation of tight reservoirs were influenced by a combination of sedimentary, diagenetic, and tectonic processes[5,18,19]. Zheng (2007) suggested that the early formation of a green clay-rich boundary with anti-compaction structure is a key factor for better reservoir properties[20]. Zhu (2015) indicated that diagenetic environments lead to the development of cementation, which causes reservoir tightness[7]. Wang (2020) argued that with increasing burial depth, the cementation process strengthens while dissolution weakens[21]. Lin (2021) and Ran (2022) believed that compaction is the main factor leading to reservoir tightness[8,22].

Current research has qualitatively characterized the controlling factors of tight reservoirs but lacks quantitative characterization of how porosity changed in each diagenetic stage affect the reservoir. Therefore, it is necessary to start from the diagenesis of tight sandstone reservoirs and the quantitative characterization of porosity, and then analyze the evolution of porosity in diagenetic stages. This conclusion is crucial for understanding hydrocarbon accumulation and target selection[23–26].

Previous research has found that the Jiamuhe Formation in the northwestern margin of the Shawan Sag consists of a set of tight sandstone reservoirs which were rich in volcanic clastic material[27–29]. The filling materials between particles were primarily zeolite cement, showing vertical zonation[29,30]. Subsequent dissolution and oil and gas charging had created reservoirs with high exploration potential[29–32]. Although Well C67, G3, and XG1 have obtained industrial gas flows from the Permian Jiamuhe Formation, quantitative studies on the compaction process and the evolution of porosity have not been conducted yet. This paper analyzes the petrological characteristics, porosity types, physical properties, and diagenesis of tight sandstone reservoirs in the Jiamuhe Formation. This study aims to restore the diagenetic evolution sequence, construct a porosity evolution model, and quantitatively calculate porosity changes under different diagenetic processes, providing theoretical support for favorable reservoir identification and target selection.

Geological setting

The study area is located in the western uplift of the Junggar Basin, at the junction of the Middle Kuai Uplift and the Hongche Fault Zone[33] (Fig. 1), consisting of fault blocks held by the Hongche Fault Zone[34,35]. The area is a southeast-tilted monoclinal structure with a 12° dip angle[36]. This region developed large-scale uplift structures during the Permian, with secondary faults forming parallel to the Hongche Fault Zone and extending into the basin[37,38]. At the end of the Permian, the area continued the early structural pattern, with sedimentary ranges gradually expanding, volcanic activity weakening, and thick coarse-grained sediments accumulating in the eastern Hongche Fault Zone[39,40]. In the Triassic, the basin underwent overall uplift and erosion, transitioning into a phase of sedimentation and uplift oscillation[37]. From the Jurassic to the Cretaceous, tectonic activities gradually weakened, with the slope area rising slowly and sedimentary conditions relatively stable[37,40]. From the Paleogene to the present, under the strong movements of the Himalayan orogeny, the Sag accumulated thick sediments[38]. The Permian in the study area consisted of the Jiamuhe Formation (P_1j), the Fengcheng Formation (P_1f), the Xiazijie Formation (P_2x), the Lower Wuerhe Formation (P_2w), and the Upper Wuerhe Formation (P_3w), with the Jiamuhe Formation primarily developing fan delta[28,41–43].

Data and methods

This study is based on a board dataset acquired and provided by the PetroChina Xinjiang Oilfield Company, which includes 23 cored wells with porosity and permeability data. In this study, the mercury injection method was used to measure porosity and permeability.

The sedimentological analysis derived mainly from data collected during the coring process is based upon the study of facies/lithofacies associations and their spatio-temporal distribution. In doing that, it is possible to recognize lithofacies and lithofacies associations, categorize boundary surfaces, deduce the sub-environments and finally define the depositional environment. The thin sections for clastic composition were achieved by Field Emission Scanning Electron Microscope (Sigma 300) in key laboratory of central Asian orogenic belts and continental dynamics.

Results

Reservoir characteristics

Lithology types and composition characteristics

In the study area, the predominant lithology type is gravelly coarse sandstone (Fig. 2), with grain sizes mainly ranging from 0.25 mm to 2 mm and overall poor sorting. The quartz content ranges from 0 to 41%, with an average of 11%. Feldspar content ranges from 1 – 59%, with an average of 25%. Rock fragments content ranges from 15 – 99%, with an average of 64%. The rock fragments were primarily volcanic clastic materials. The compositional maturity index (Q/(F + R)) ranges from 0 to 0.7, with an average of 0.14, indicating extremely low compositional maturity. The rocks are mainly classified as lithic sandstones and include lithic feldspar sandstone and feldspar lithic sandstone (Fig. 3a and b), reflecting a proximal sedimentary environment. Analysis of thin sections from 286 samples across 14 wells in the study area shows that the highest content of cementing materials is zeolite, at 3.91%, followed by carbonate cement, with an average content of 2.39%. The average content of
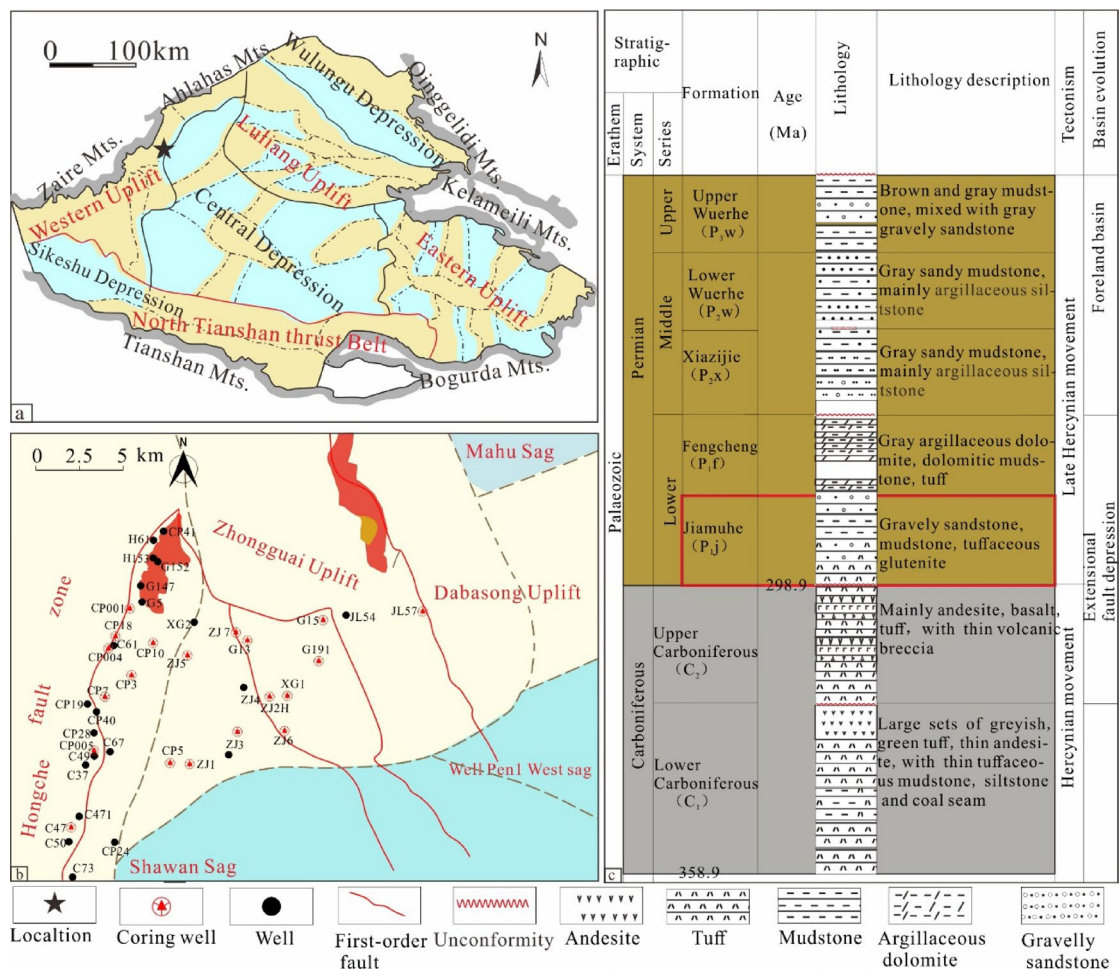
Fig. 1. Structural of the northwest margin of Shawan Sag, Junggar Basin. (**a**) The location of the study area within the Junggar Basin. (**b**) The location of the study area. (**c**) Comprehensive columnar diagram of the western margin of Shawan sag. The figures a-c were created by the Geomap v4.0 software (https://www.geomapapp.org).
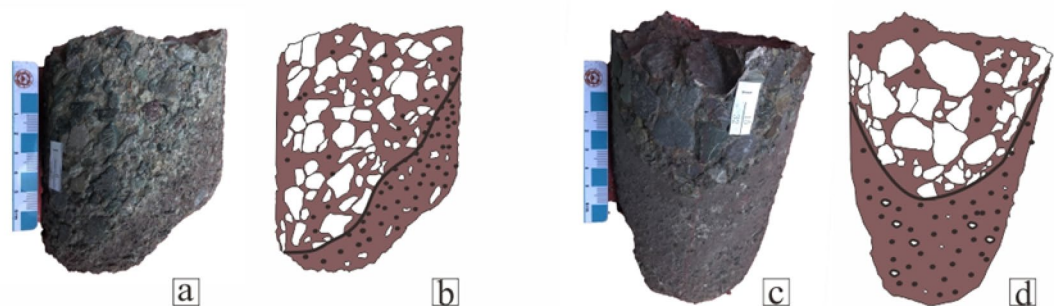

Fig. 2. Core photos of the Jiamuhe Formation in the northwest margin of Shawan Sag, Junggar Basin. (**a**) CP28, 2139 m. (**b**) the lithology sketch of **a**. (**c**) CP19, 2141 m. (**d**) The lithology sketch of **c**.

mixed matrix is 1.15%, predominantly consisting of tuffaceous matrix. The average content of clay cement is 0.23% (Fig. 3b and b).

Pore types
In the study area, the pore types were mainly secondary pores, with localized development of microfractures. Influenced by dissolution processes, secondary pores include moldic pores (Fig. 4a), interstitial dissolution pores
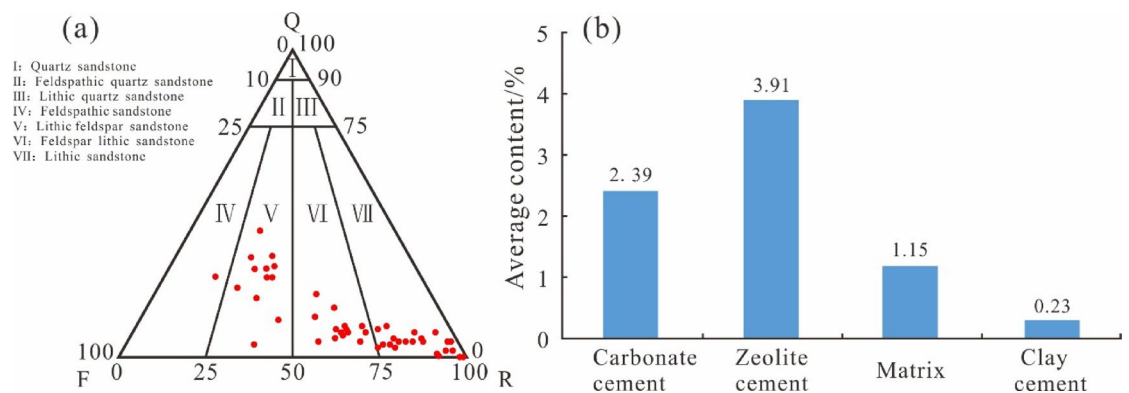
Fig. 3. Petrographic characteristics of the Jiamuhe Formation in the Northwest margin of the Shawan Sag. (**a**) triangulation diagram of rock types and histogram. (**b**) types of intergranular filling materials.
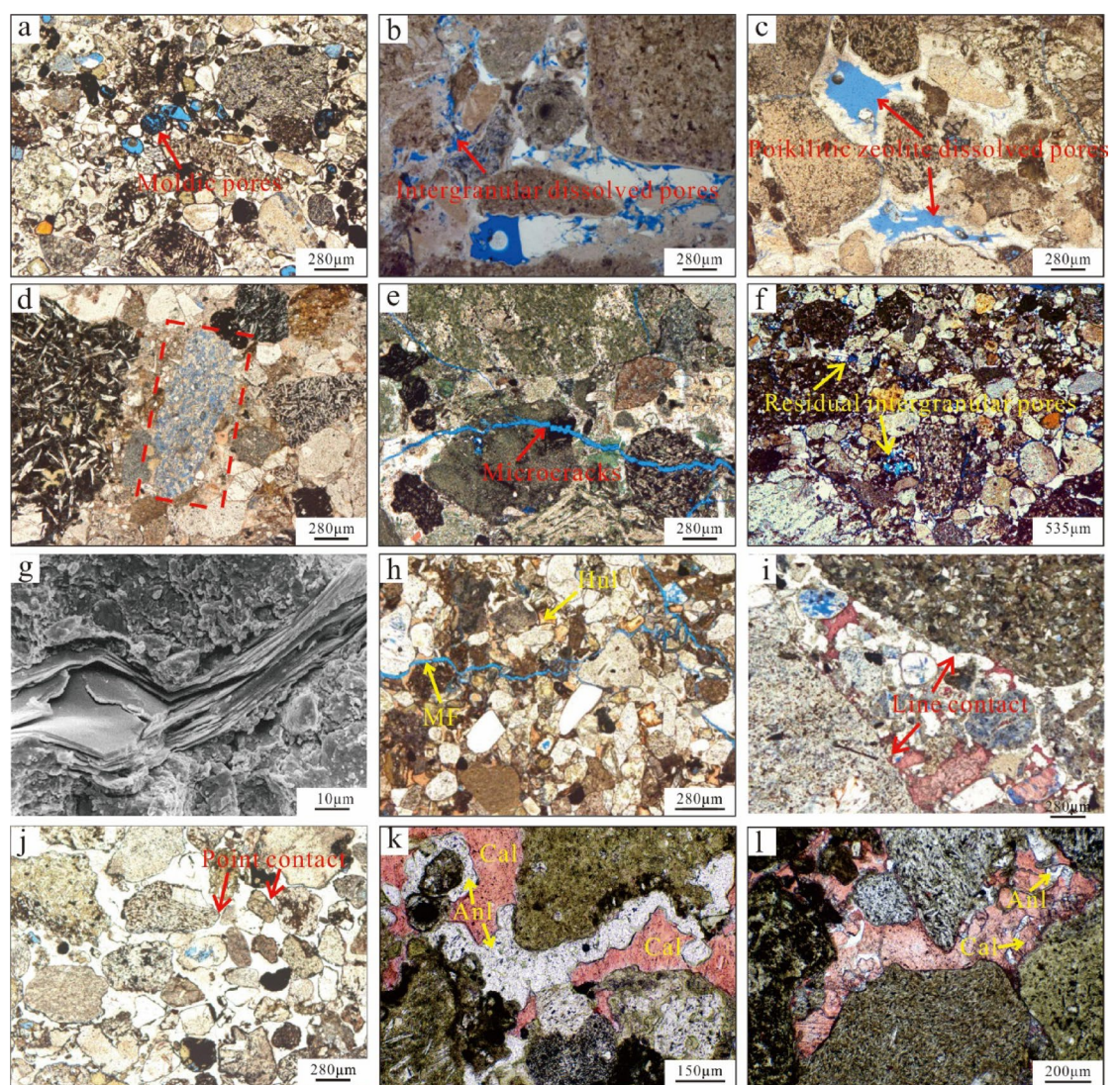

Fig. 4. Thin slice pore types of tight sandstone reservoirs in Jiamuhe Formation, northwest margin of Shawan Sag. (**a**) Well ZJ 4, 4406.87 m, ×50, (-). (**b**) Well CP 001, 2473 m, ×50, (-). (**c**) Well ZJ 4, 4637.36 m, ×50, (-). (**d**) Well Hong 153, 2735.58 m, ×50, (-). (**e**) Well ZJ 6, 4956.53 m, ×50, (-). (**f**) Well ZJ 1, 4859.59 m, ×50, (-). (**g**) Well CP 7, 3421.00 m, ×50, (-). (**h**) Well CP 10, 3496.09 m, ×50, (-). (**i**) Well CP 21, 2691.5 m, ×50, (-). (**j**) Well ZJ 4, 4412.46 m, ×50, (-). (**k**) Well CP 005, 2972.30 m, ×50, (-). (**l**) Well CP 002, 2775.1 m, ×50, (-).

(Fig. 4b), zeolite dissolution pores (Fig. 4c), intra-granular dissolution pores (Fig. 4d), microfractures (Fig. 4e), bent mica fragments (Fig. 4g), playing a constructive role in improving the reservoir's storage and performance. Residual intergranular pores persisted despite the effects of compaction and cementation (Fig. 4f).

Physical property variation characteristics
Analysis of porosity data from 1163 samples across 23wells in the Jiamuhe Formation reveals the following: the porosity ranges from 6 − 16%, with 77.7% of the samples falling within this range. The permeability ranges from (0.1–1) mD, with 27.6% of the samples showing permeability in this range. Overall, the Jiamuhe Formation reservoirs were classified into low-porosity, ultra-low-permeability tight sandstone reservoirs[43–45].

Further analysis showed that the correlation between porosity and permeability in the Jiamuhe Formation is poor, with obvious zoning and zonation (Fig. 5). The study area developed a fan delta[46] (Fig. 6a). There were 173 samples with porosity greater than 15%, and 510 samples with permeability ranging from 0.01 mD to 1 mD in delta plain facies (Fig. 6b and d). The delta plain facies were characterized by "low to medium porosity and extra to ultra-low permeability". There were 85 samples with porosity greater than 15%, and 290 samples with permeability in the range of 1 to 50 mD (Fig. 6c and e), and show a characteristic of "low porosity, extra to medium-high permeability" in the delta front facies.

Diagenesis types and characteristics
Compaction
In delta plain, the linear contact (Fig. 4i) and bent mica fragments (Fig. 4g) were developed, indicating substantial loss of primary porosity. While in delta front, in areas away from the overthrust belt of the Hongche fault zone, the contacts between particles were mainly point contact (Fig. 4j), preserving a small amount of primary residual intergranular porosity (Fig. 4f).
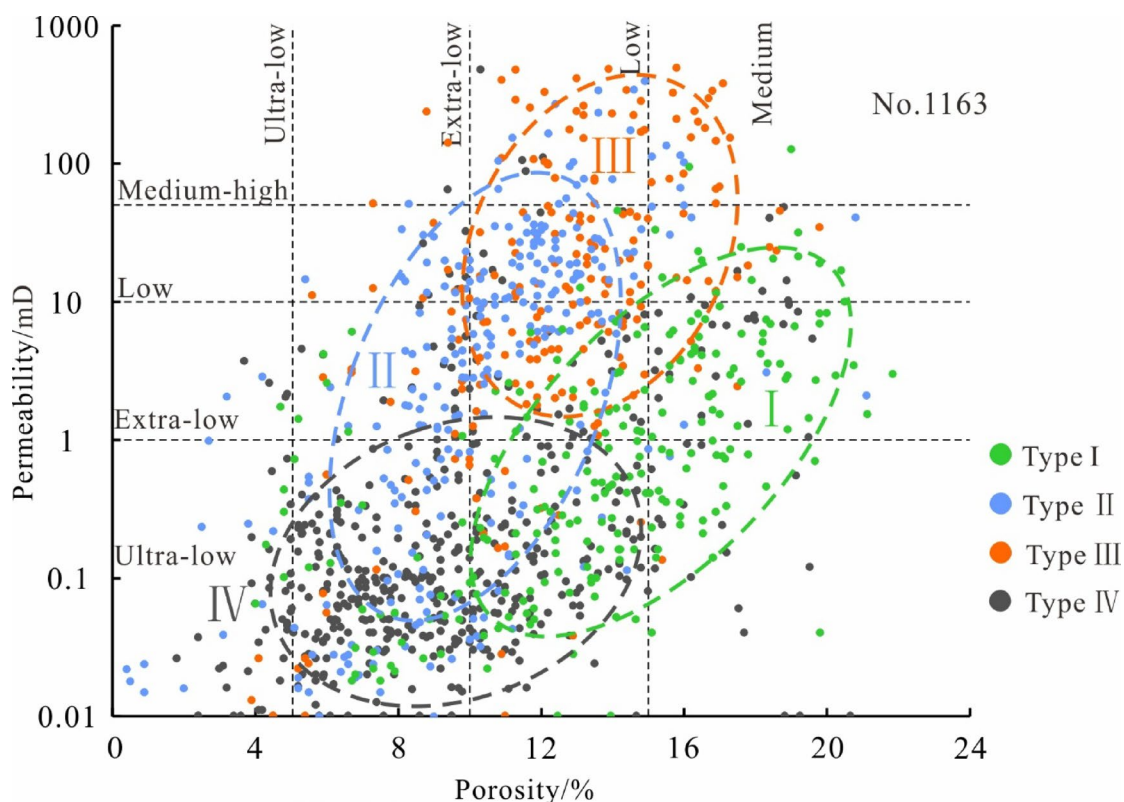

Fig. 5. Porosity-Permeability Cross-Plot of the Jiamuhe Formation in the Northwest Margin of the Shawan Sag. The classification and distribution of porosity and permeability data are as follows. Type I porosity ranges from 10 − 20% with permeability ranges from (0.1–10) mD, It exhibits medium porosity, low to ultra-low permeability, and located in the Well CP21 area. Type II is porosity ranges from 5 − 14% with permeability ranges from (0.5–50) mD. It exhibits low porosity, extra to low permeability, and located in the Well ZJ 5 area. Type III is porosity ranges from 10 − 18% with permeability ranges from (1–500) mD. It exhibits extra-low porosity, medium-high to extra-low permeability, and located in the Well ZJ 6 area. Type IV is porosity ranges from 4 − 12%, permeability ranges from (0.01–1) mD. It exhibits ultra-low porosity, extra to ultra-low permeability, and located in the Well CP 004 area.
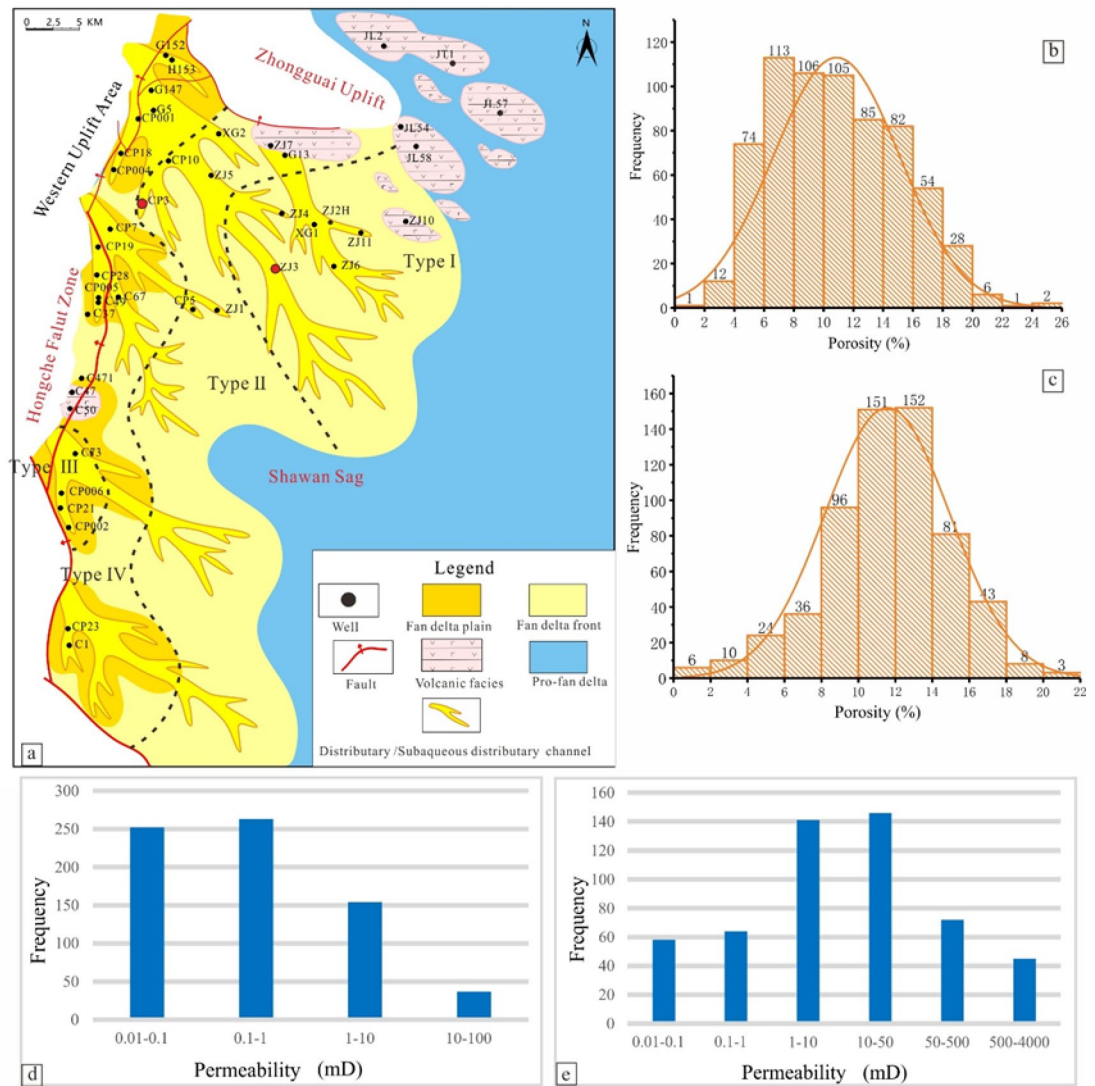
Fig. 6. Sedimentary facies and porosity-permeability zonation map of the Jiamuhe Formation in the Shawan Sag. (**a**) sedimentary facies. (**b**) porosity distribution of the delta plain. (**c**) porosity distribution of the delta front; d. permeability distribution of the delta plain facies. (**e**) permeability distribution of the delta front. The figures were created by the Geomap v4.0 software (https://www.geomapapp.org).

Cementation

Cementation in the Jiamuhe Formation includes zeolitic cement, carbonate cement, and clay mineral cement. Among these, zeolitic and carbonate cement is relatively more prevalent (Fig. 7).

Zeolite cement   The formation of zeolitic minerals in the Jiamuhe Formation is closely related to volcanic materials and is a widespread cement type in the area[30,47]. Analysis of cement content reveals that in the plain facies mainly developed porous-type heulandite (Fig. 4h), accompanied by a small amount of analcite and dolomite. In the eastern ultra-deep subsurface, the main cement was mosaic-type laumontite (Fig. 4j). From the delta plain facies to the front facies, the content of laumontite increased, enhancing the compaction resistance of the framework particles (Fig. 4k), and improving porosity progressively.

Carbonate cement   The carbonate cement in the region was primarily composed of calcite, with an average content of 2.36%, and accompanied by a small amount of dolomite. Calcite appeared as an interstitial filling in the residual intergranular pores (Fig. 4k) and occasionally replaces analcime (Fig. 4l). The formation period of calcite was generally later than that of analcime. The conversion of clay minerals and dissolution of volcanic-rock fragments during the eodiagenesis provided the material basis for the formation of calcite[7,47].

The presence of carbonate cement indicated a dual impact on the reservoirs development. On one hand, carbonate cementation occluded pores, significantly reducing the porosity and permeability of sandstone. On the other hand, the deposition of cement supported the reservoir texture, minimizing the degree of compaction
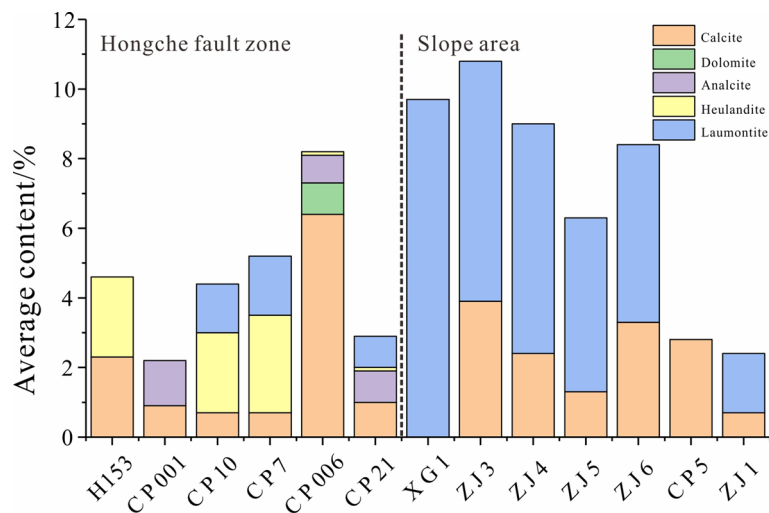
Fig. 7. The average content of reservoir cement in Jiamuhe Formation, Shawan Sag. The Hongche fault zone is surrounded by delta plains, while the slope area is mainly developed the delta front.
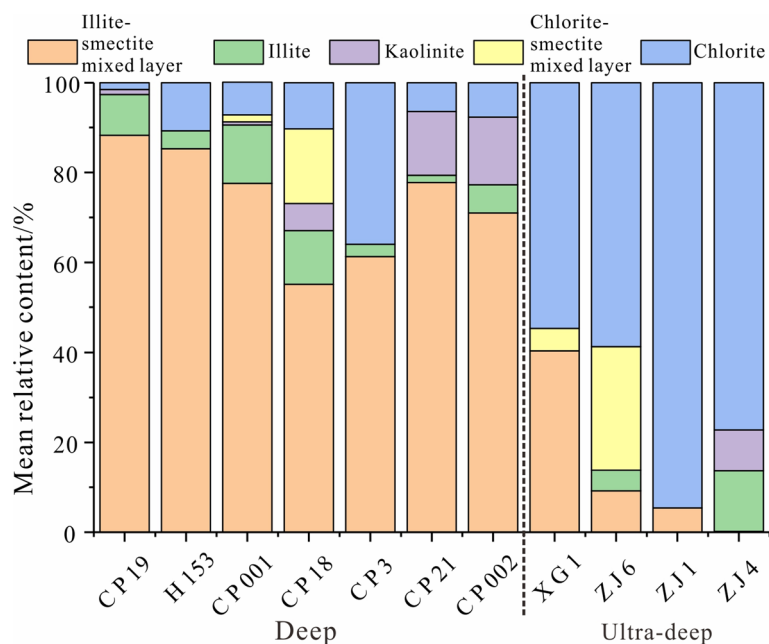

Fig. 8. The average relative content of authigenic clay minerals in Jiamuhe Formation, Shawan Sag.

in the sandstone and creating favorable conditions for subsequent acidic dissolution, which led to the formation of secondary porosity.

Clay mineral cement   Through statistical analysis of X-ray diffraction (XRD) data from 123 samples across 11 wells in the region (Fig. 8), it was observed that the dominant clay mineral type in the Jiamuhe Formation was illite-smectite mixed layer, with an average relative content of 42.77%. The volcanic materials buried at shallow depths in the slope zone had undergone hydrated reactions due to atmospheric and groundwater infiltration. This led to the formation of a potassium-rich environment, which favored the transformation of smectite into illite-smectite mixed layer. Additionally, this process generated many alkaline cations, providing the material basis for carbonate and zeolite cementation, thereby enhancing the degree of later cementation[47,48]. The relative content of chlorite was second only to illite-smectite mixed layer, averaging 38.15%. There were two primary modes of chlorite formation in the reservoir[48]. Deep Burial Transformation: chlorite formed from the transformation of chlorite-smectite mixed layer into chlorite due to deep burial. Chlorite develops as a leaf-like structure on particle surfaces, forming chlorite rims with resistance to compaction. The results in favorable petrophysical properties in the fore-slope area represented by the Well ZJ zone[20]. Alkaline Ion Contribution: during the

transformation of smectite to illite-smectite mixed layer, the alkaline ions released contribute to the formation of chlorite. This characteristic was found in the plain facies represented by the Well CP zone. However, the low degree of chlorite development in this area suggested that it did not exhibit strong resistance to compaction.

The impact of authigenic clay minerals on reservoir properties was complex. Chlorite films growing along the edges of detrital grains and kaolinite cements filling pore spaces typically occupied effective reservoir space and disrupt pore connectivity. However, irregularly shaped chlorite films growing vertically along pore walls inhibited the growth of secondary quartz or feldspar edges. Meanwhile, kaolinite aggregates filling pores provided a material basis for dissolution processes, which was beneficial for the formation of secondary porosity.

Dissolution processes
Dissolution of rock layers had been influenced by the Hercynian orogeny and atmospheric water infiltration[28–30,32,47]. As burial depth increased, deeper reservoir rocks experienced dissolution impacts from organic acids, which were significantly stronger than the dissolution effects from atmospheric fresh water[29,30]. In this study, easily soluble components within detrital particles were dissolved, creating intragranular pores (Fig. 4d). Some of these dissolution processes led to the formation of moldic pores (Fig. 4f). The dissolution of zeolite-type cement, which was predominant in certain areas, results in the creation of numerous dissolution pores (Fig. 4c). This effect was particularly pronounced in regions with higher zeolite content, such as the Well ZJ zone. The secondary porosity created by these dissolution processes significantly enlarged the pore space in the reservoir, thus playing an important constructive role in enhancing reservoir quality.

Structural fracturing
The Jiamuhe Formation had been influenced by structural activities such as the Hongche fault zone. These tectonic activities had resulted in the widespread development of micro-fractures (Fig. 4e and h). These micro-fractures significantly improved the connectivity of the reservoir space and played an important role in enhancing the reservoir performance of the Jiamuhe Formation[32,49]. Specifically, the formation of these fractures increased the reservoir's porosity and permeability, allowing fluids to migrate and be stored more effectively within the reservoir.

Discussion
Diagenetic stages and sequences
The Jiamuhe Formation showed gas-liquid two-phase hydrocarbon inclusions with fluorescence colors generally being yellow, and some cementation material showing blue, indicating higher oil and gas maturity[50–52]. Fluorescence under blue light revealed blue fluorescence at the edges of detrital grains and in intergranular pores (Fig. 9).

Homogenization temperature tested from 8 wells in the Jiamuhe Formation reveal two peak regions. The carbonate cementation in the delta plain facies, such as in Well CP 7, formed within a main temperature range of 65–105 °C. This was largely due to early-forming calcite cementation, which partially inhibits further compaction of the sandstone and suppresses the filling of authigenic clay minerals. In the delta front facies, such as in Well CP5, the homogenization temperature ranges of inclusions obtained from quartz host minerals was 85–135 °C (Fig. 10). Combining the inclusions and homogenization temperature data indicated two phases of oil and gas charging in the study area.

In the study area, the sequence of cement and authigenic minerals is as follows: chlorite → calcite → illite-smectite mixed-layer minerals → analcime → phillipsite → clinoptilolite. Combining the homogenization temperature data from inclusions with the diagenetic stages and the cement and authigenic mineral sequence, the diagenetic stages were mainly from eodiagenesis stage B to mesodiagenesis A. Based on the chronological order of diagenetic events, the sequence was: compaction → chlorite coating → calcite cementation → illite/smectite mixed-layer minerals → sheet-like chlorite → analcime cementation → phillipsite cementation → clinoptilolite cementation → dissolution → localized fracturing (Fig. 11).

Quantitative characterization of pore evolution
Based on the diagenetic analysis, the pore evolution of Jiamuhe Formation sandstones was quantified as follows. This approach helped to restore the pore evolution of compacted sandstones through different diagenetic stages.

Calculation of initial porosity
The φ_0 can be calculated using the formula proposed by Beard and Weyl for unconsolidated sandstones with different sorting conditions[53,54]:

$$\phi_0 = 20.91 + 22.90/S_o$$

For the Jiamuhe Formation reservoirs, the Trask sorting coefficient(So)ranges from 1.01 to 3.84, with an average of 2.15. Based on this, the initial porosity of the target interval is calculated to be between 26.87% and 43.58%, with an average of 32.79%.

Compaction-induced porosity reduction calculation
φ_1 refers to the remaining unfilled intergranular pores after the eodiagenesis A compaction and cementation. It can be calculated by using the relationship between the cement content, the intergranular pore surface porosity, and the petrophysical analysis porosity. The formula is,
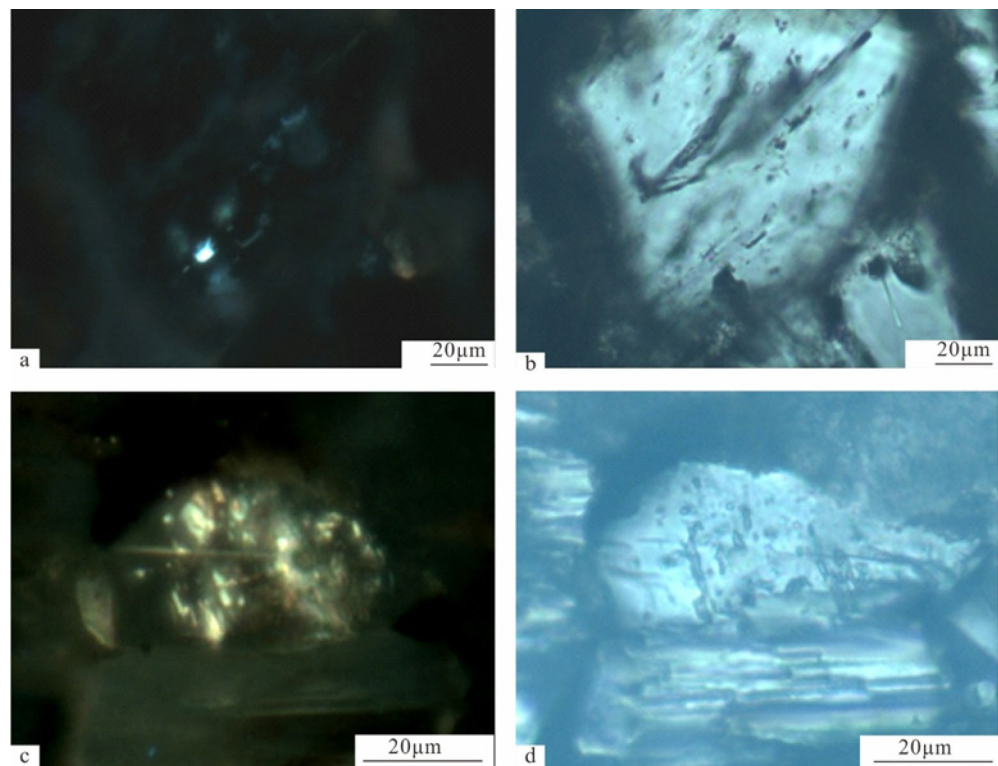
Fig. 9. Hydrocarbon inclusion characteristics of Jiamuhe Formation in Shawan Sag. (**a**) Well CP 7, fluorescence, oil and gas inclusions, 3421 m. (**b**) the same field of view as **a**, transmitted light. (**c**) Well CP5, fluorescence, oil and gas inclusions, 4733.22 m. (**d**) in the same field of view as **c**, transmitted light.
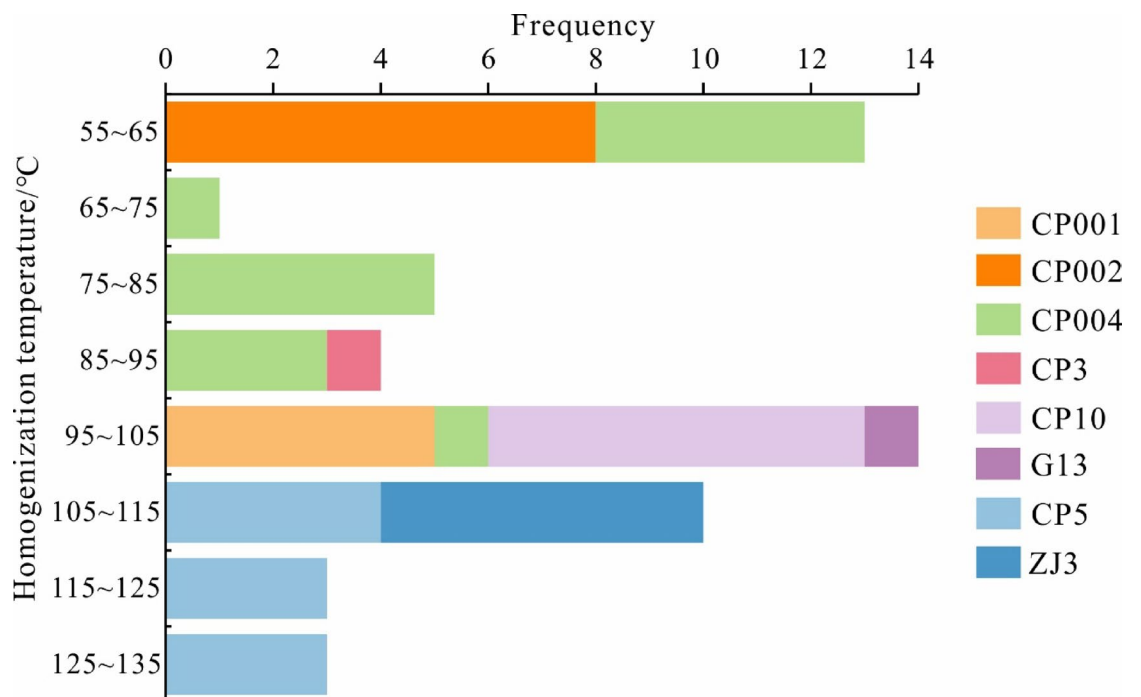

Fig. 10. Frequency distribution of homogenization temperature for quartz and calcite cements in Jiamuhe Formation, Shawan Sag.
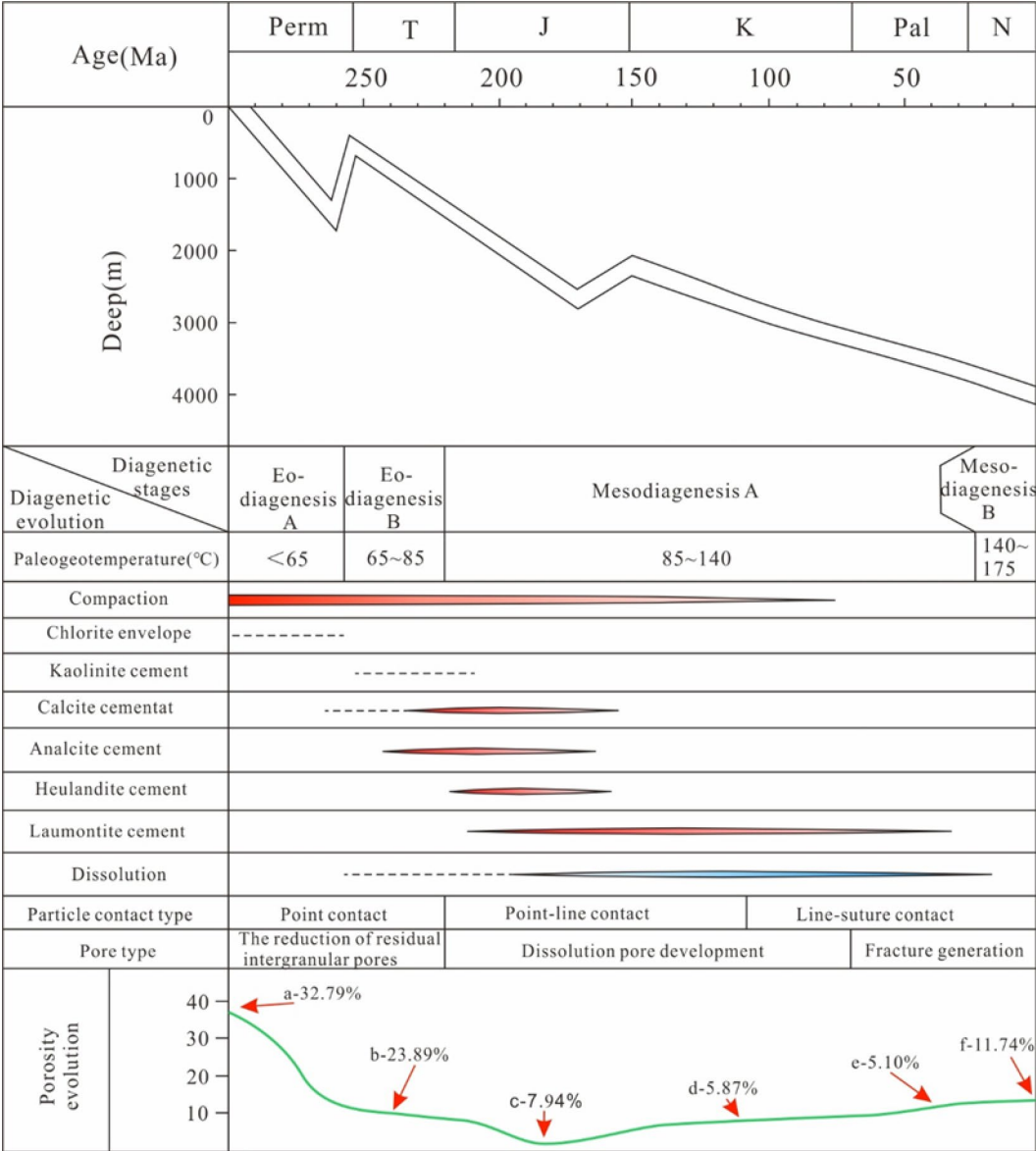
Fig. 11. Diagenetic sequence and pore evolution model of sandstone reservoir of Jiamuhe Formation in Shawan Sag. Note: (a) Initial porosity. (b) Compaction-induced porosity reduction. (c) Cementation-induced porosity reduction. (d) Dissolution-induced porosity increase (e) Microfracture-induced porosity increase; f. Final porosity.

$$\phi_1 = \frac{a_1}{a} \times p + V_c$$

$$\phi_2 = \phi_0 - \phi_1$$

$$R_p = \phi_2 \times 100 / \phi_0$$

For the Jiamuhe Formation sandstones, compaction reduced the porosity from 32.79 to 8.90%, resulting in a compaction reduction rate of 72.86%.

Based on the quantification of the degree of compaction and the integration of the differences in porosity evolution among different well areas, the trend lines of the blue point (Well CP 21 area) and the yellow point (Well CP 004 area) were approximately parallel and showed relatively large slope (Fig. 12a), indicating that the porosity rate decreased with the enhancement of compaction; the trend lines of the orange point (Well ZJ 5 area) and the gray point (Well ZJ 2 H area) were approximately parallel but showed smaller slope (Fig. 12a), and the influence of compaction on the reservoir properties was less than that of the points in the Well CP areas.
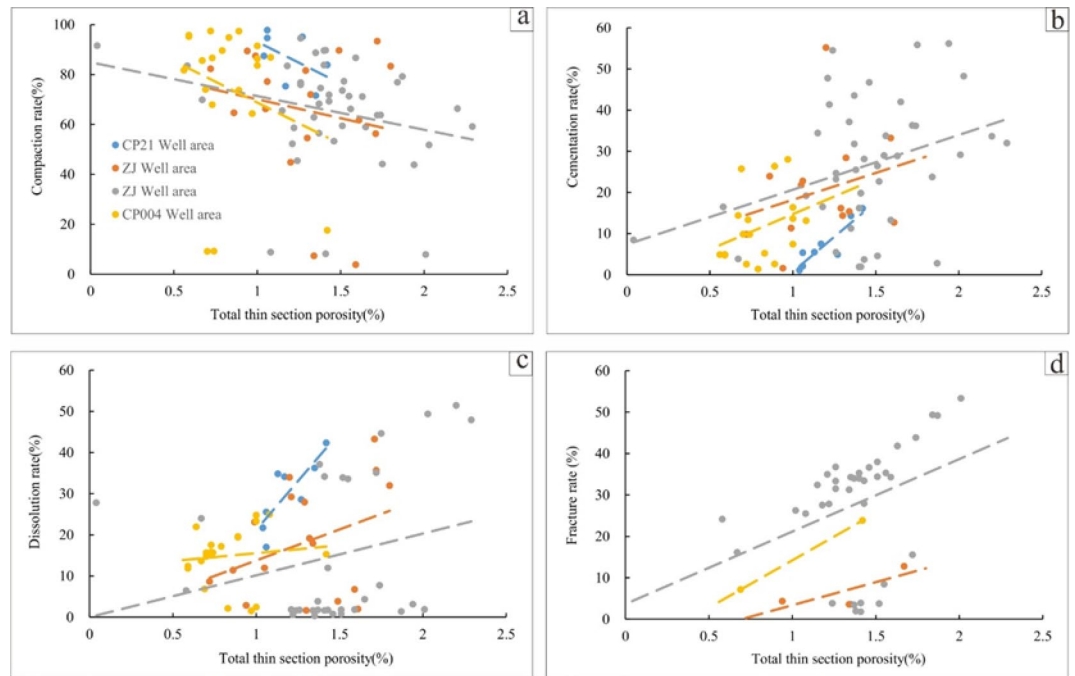
Fig. 12. The correlation between the total thin section porosity and diagenesis. (**a**) the correlation between the total thin section porosity and compaction ratio. (**b**) the correlation between the total thin section porosity and cementation ratio. (**c**) the correlation between the total thin section porosity and dissolution ratio. (**d**) the correlation between the total thin section porosity and fracture ratio. The legend for **b ~ d** is the same as that for **a**.

Cementation-induced porosity reduction calculation
During the eodiagenesis A, the amount of cementation material was relatively low, the primary porosity loss due to cementation occurs during the eodiagenesis B. Thus, φ_3 represents the residual intergranular pores that were not filled by cementation material during the eodiagenesis B. The formula for calculating φ_3 is,

$$\phi_3 = \frac{a_1}{a} \times p$$

$$\phi_4 = \phi_1 - \phi_3$$

$$R_c = \phi_4 \times 100/\phi_0$$

For the study area sandstones, the calculations yield the following results, φ_3 is 0.96%. φ_4 is 7.94%. The cementation reduction rate (R_c) is 24.21%.

Based on the above quantitative analysis of the degree of cementation and the comprehensive consideration of the differences in porosity evolution among different well areas, the overall trend line of the points in the study area generally shows that the total thin section porosity increases with the strengthening of cementation (Fig. 12b), indicating that the cementation effect has a stronger inhibitory ability on compaction than on reducing porosity. Based on the analysis of the compositional rock characteristics and tectonic activity characteristics of Jiamuhe Formation, it is believed that the reservoir cementation content in the Well CP area of the Hongche Fault Zone is low, with an average content of 4.6% (Table 1), and its ability to resist compaction is relatively weak, while in the Well ZJ area of the depression, the reservoir cementation content is relatively high, with an average content of 7.1% (Table 1), significantly enhancing the later compaction resistance ability of the reservoir.

Dissolution-induced porosity increase calculation
ϕ_5 from secondary dissolution pores formed during the acidic dissolution faces in the eodiagenesis A is given by,

$$\phi_5 = \frac{a_2}{a} \times p$$

$$R_1 = \phi_5 \times 100/\phi_0$$

For the studied tight sandstone reservoirs, φ_5 is 5.87%, and the dissolution rate (R_1) is 17.90%.

Based on the above quantitative analysis of the degree of dissolution and the comprehensive consideration of the differences in porosity evolution among different areas, it was found that the trend line slope at the blue point (Well CP 21 area) was relatively large, and the porosity rate increased significantly with the increase of

Well	Cementation		Cementation		Dissolution		Structural fracturing	
	Porosity loss(%)	Porosity loss rate(%)	Porosity loss(%)	Porosity loss rate(%)	Porosity gain(%)	Porosity gain rate(%)	Porosity gain(%)	Porosity gain rate(%)
H153	25~39 (33)	66~97 (88)	1~13 (5)	3~34 (12)	5~7 (6)	12~19 (16)	0~0 (0)	0~0 (0)
CP001	19~34 (30)	59~97 (82)	1~7 (3)	3~22 (11)	4~8 (7)	12~22 (18)	0~0 (0)	0~0 (0)
CP 10	29~31 (30)	73~85 (77)	5~31 (15)	15~28 (23)	3~10 (7)	7~28 (18)	0~9 (2)	0~7 (2)
CP 7	26~32 (28)	81~94 (86)	2~6 (5)	6~19 (14)	6~9 (8)	19~29 (24)	0~0 (0)	0~0 (0)
CP 21	23~40 (34)	72~97 (88)	1~7 (4)	0~18 (9)	11~21 (14)	25~56 (39)	0~0 (0)	0~0 (0)
ZJ1	14~26 (20)	46~85 (65)	4~9 (6)	13~27 (22)	1~11 (5)	2~33 (18)	0~0 (0)	0~0 (0)
ZJ 4	10~27 (19)	34~90 (64)	3~20 (11)	10~66 (36)	0~18 (10)	0~60 (34)	0~17 (7)	0~59 (25)
ZJ 5	5~30 (18)	16~88 (58)	4~19 (9)	12~66 (29)	2~12 (7)	8~41 (23)	0~5 (1)	0~15 (6)
ZJ 6	12~30 (21)	37~94 (67)	2~20 (10)	6~63 (33)	0~4 (1)	1~14 (3)	6~18 (12)	19~64 (39)

Table 1. Quantitative analysis of diagenetic porosity loss or gain for different well in the Jiamuhe formation reservoir. Note: Values in parentheses represent the average.

dissolution rate. This indicates that the developed dissolution effect had a positive significance for improving the reservoir space. At the yellow point (Well CP 004 area), the main pore type was intragranular dissolution pores, and the total thin section porosity showed a slight upward trend with the increase of dissolution degree. The reservoir physical properties of this area have been improved to a lesser extent due to the dissolution effect. At the gray point (Well ZJ 2 H area), there was a significant numerical difference on both sides of the trend line. The main reason was that this well area was in the development area of tectonic movement, where many micro-fractures were formed, enhancing the connectivity of the reservoir space and making the dissolution effect of acidic fluids developed more (Fig. 12c).

Microfracture-induced porosity increase calculation
ϕ_6 is attributed to secondary porosity developed due to stress during the late diagenetic stage. The calculation is given by:

$$\phi_6 = \frac{a_3}{a} \times p$$

$$R_2 = \phi_6 \times 100/\phi_0$$

For the study area tight sandstone reservoirs, ϕ_6 is 5.10%, and the microfracture increase rate (R_2) is 15.55%.

Based on the above quantitative analysis of the degree of fractures and the comprehensive consideration of the differences in porosity evolution among different well areas, it was found that the number of yellow points (in the Well CP 004 area) and orange points (in the Well ZJ 5 area) was relatively small, indicating that the degree of tectonic activity was relatively low; the gray points (in the Well ZJ 2 H area) had a relatively good correlation between the porosity rate and the fracture rate, suggesting that the porosity rate increases with the formation of micro-fractures, thereby improving the connectivity of the reservoir space (Fig. 12d).

Porosity evolution
Based on the previous analysis and calculations, the porosity evolution in the study area had undergone several diagenetic stages. Eodiagenesis A, during rapid deposition and burial, the Jiamuhe Formation experienced significant compaction. Illite films grew on particle edges, and minor calcite cement filled intergranular pores, heavily influencing reservoir properties through compaction. Eodiagenesis B, a significant tectonic uplift led to weathering of rock fragments and clay minerals at the top of the Jiamuhe Formation. This weather released alkaline ions, and with rising temperatures due to geothermal gradients, calcareous cements began to fill the pores. Compaction further reduced porosity from an original 32.79% to about 8.90%. Mesodiagenesis A, as burial depth increased to around 3000 m, carbonate and zeolite cement intensified, forming mainly calcite, calcic zeolites, phyllosilicates, and cloudy zeolites within pores, further reducing porosity. Cementation reduced porosity by 7.94%. Later, organic acids and oil-gas charging caused late dissolution, increasing porosity by 5.87%. Local structural effects led to microfractures, increasing porosity by 5.10%. Currently, the porosity is approximately 11.74% (Fig. 11). Overall, the theoretical results align well with the peak values of physical property distributions, providing a theoretical basis for evaluating and exploring the Jiamuhe Formation reservoirs in the northwestern edge of the Shawan Sag.

Diagenetic Intensity	Compaction-Driven Porosity Reduction (%)	Cementation-Driven Porosity Reduction (%)	Dissolution-Induced Porosity Increase (%)	Fracture-Induced Porosity Increase (%)
Strong	≥ 75	≥ 20	≥ 25	≥ 10
Moderate	50 ~ 75	10 ~ 20	15 ~ 25	1 ~ 10
Weak	< 50	< 10	< 15	< 1

Table 2. Division of different types of action intensity of Jiamuhe formation in Shawan sag.
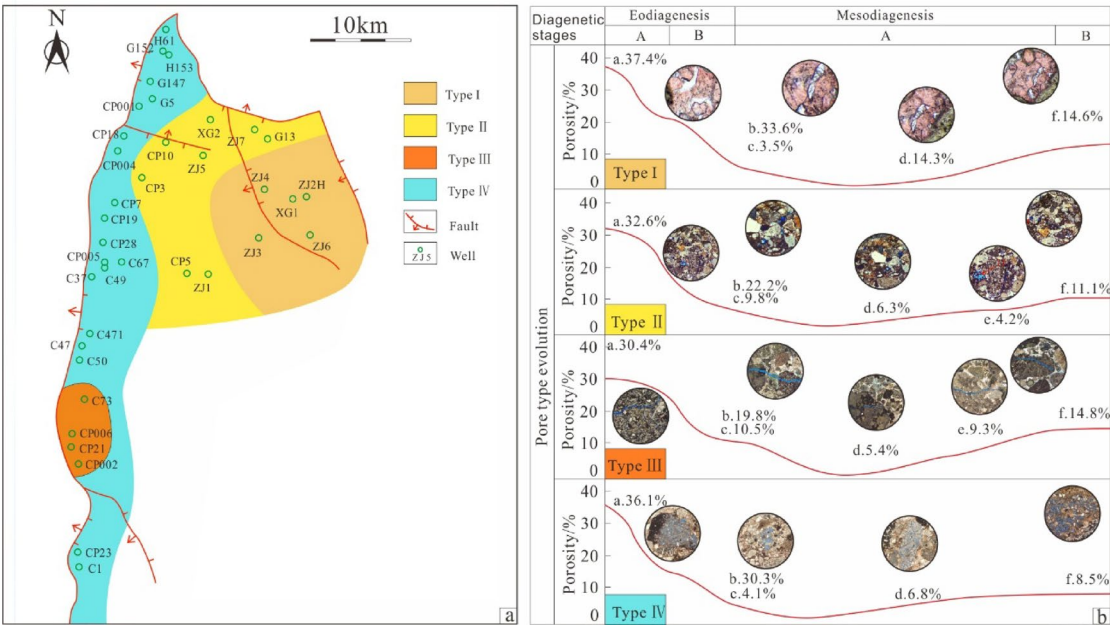

Fig. 13. Diagenetic facies distribution map of Jiamuhe in the northwest margin of Shawan Sag. Notes correspond to Fig. 11. Note. (**a**) Diagenetic facies distribution map. (**b**) Evolution of pores in different diagenetic stages. The figures were created by the Geomap v4.0 software (https://www.geomapapp.org).

Diagenetic facies

Diagenetic facies represented the products of sedimentary materials undergoing diagenetic evolution under specific conditions[55]. Due to the variability of geological conditions in different regions, a unified standard for diagenetic facies classification cannot be established[6,22,55]. Therefore, this study quantitatively analyzes porosity changes under the influence of various diagenetic processes (Table 1) and classifies the intensity of diagenetic facies into three levels: strong, moderate, and weak (Table 2).

The diagenetic facies were classified based on the cementation-sedimentation-pore type. These classifications, depicted in Fig. 13, help in understanding the spatial variations in diagenetic processes and their effects on porosity, providing a basis for more detailed reservoir characterization and exploration strategies in the Jiamuhe Formation.

Strong cementation – outer zone of front delta-dissolution pores facies (type I, ZJ 6 well area)
These diagenetic facies were minimally affected by the Hongche thrust fault zone. Although the reservoir was buried relatively deep, the compaction effect was relatively weak, with a compaction-induced porosity reduction of about 19.8%. Lithology was primarily feldspar sandstone. The extensive development of zeolite and chlorite cement further enhanced the resistance of the particle framework to compaction, with a cementation-induced porosity reduction of about 10.5%. Dissolution pores formed under the influence of organic acids and microcracks created by structural fracturing resulted in a cumulative porosity increase of about 14.7%. These secondary pores not only provided additional storage space, but also enhanced the connectivity between pores. Meanwhile, the ZJ6 Well area developed a nose-shaped structure. The central part of this structure formed opening-type micro-cracks under the tensioning effect, which improved the reservoir's permeability. This diagenetic facie was mainly located at the Well ZJ6 location in the outer zone of the delta front, and it represented favorable diagenetic facies.

Strong cementation – Inner zone of the delta front-Intra granular dissolution pores moderate dissolution facies (type II, ZJ 5 well area)
These diagenetic facies were moderately affected by thrust faulting. The compaction-induced porosity reduction was about 22.2%. The lithology of type II was mainly feldspar lithic sandstone, with abundant crystal-embedded zeolite cement, resulting in a cementation-induced porosity reduction of about 9.8%. This enhanced the reservoir's resistance to compaction and preserves some residual intergranular pores. Some lithic particles were dissolved by acidic fluids, forming intragranular dissolution pores and mold pores, leading to a secondary porosity increase of about 10.5%, which benefited oil and gas storage. This diagenetic facie was mainly located at Well the ZJ5 location in the inner zone of the delta front.

Weak cementation –delta plain -intergranular dissolution pores strong facies (type III, CP21 well area)
These diagenetic facies were primarily controlled by the thrust faulting of the Hongche Fault Zone. It consisted mainly of lithic sandstone. The rocks were initially affected by strong compaction, with a porosity reduction of about 33.6%. The cements were predominantly carbonate with some feldspathic zeolite, causing a cementation-induced porosity reduction of about 3.5%, which prevented further damage from compaction. Dissolution of soluble components like carbonates has improved the reservoir properties, resulting in a porosity increase of about 14.3%. This diagenetic facie was mainly located at the Well CP21 location in the inner zone of the delta front. It represents favorable diagenetic facies type.

Strong compaction – delta plain-intergranular dissolution pores moderate cementation facies (type IV, CP004-C37 well area)
These diagenetic facies were primarily feldspathic lithic sandstone, heavily influenced by late Hercynian thrust faulting. Despite relatively shallow burial depth, compaction was significant, reducing porosity by about 30.3%. The pores were filled mainly with feldspathic zeolite cement, reducing porosity by about 4.1%, which set the stage for dissolution processes. Dissolution by organic acids increased porosity by about 6.8%. This diagenetic facie was mainly located at the Well CP004-C37 area location in the delta plain.

Based on diagenetic analysis and strength classification, the distribution of diagenetic facies in the study area was mapped using dominant facies analysis (Fig. 12). Strong mechanical compaction near the Hongche Fault Zone has led to significant compaction and the development of soluble components, showing favorable physical properties. Towards the central Shawan Sag, cementation becomes more pronounced, with local faulting enhancing reservoir connectivity.

Conclusion

(1) The tight sandstone reservoirs of the Jiamuhe Formation on the northwest margin of the Shawan Sag was primarily composed of lithic sandstones. The structural and compositional maturity was relatively low. The pore types were mainly intragranular dissolution pores and zeolite dissolution pores, and microfractures were developed locally. Along the Hongche fault zone, compaction was relatively strong, and in the slope area, zeolite cementation was manifested. Local dissolution and structural fracturing had improved reservoir properties, and the overall characteristics were medium-low porosity and medium-low permeability.

(2) The diagenetic stages in the study area ranged from early diagenetic stage B to middle diagenetic stage A. The diagenetic evolution successively experienced compaction→early chlorite coating→early meteoric water dissolution→early calcite/kaolinite cementation→middle-stage analcime/philipsite/zeolite cementation →middle-stage organic acid dissolution→microfractures.

(3) The porosity of the Jiamuhe Formation reservoirs in the Shawan Sag changed during diagenesis. The porosity in the early diagenetic stage decreased from the original 32.79% to about 8.9%, and further decreased to about 0.96% in the middle diagenetic stage A. The dissolution effect of organic acids increased the porosity to about 6.83%, and the porosity increased to about 11.74% at present due to the improvement by tectonic stress. Four diagenetic facies can be identified: (1) Strong Cementation - Outer zone of front delta - Dissolution pores facies. (2) Strong cementation - Inner zone of the delta front - Intra granular dissolution pores moderate dissolution facies. (3) Weak cementation - Delta plain - Intergranular dissolution pores strong facies. (4) Strong compaction - Delta plain - Intergranular dissolution pores moderate cementation facies.

Where

S_o is the Trask sorting coefficient, $S_o = (P_{25}/P_{75})^{1/2}$, P_{25} is the particle diameter at the 25% cumulative point on the distribution curve. P_{75} is the particle diameter at the 75% cumulative point on the distribution curve.

ϕ_0 = initial porosity
$\varphi 1$ = remaining intergranular porosity after compaction,
ϕ_2 = porosity loss due to compaction
ϕ_5 = *porosity increase due to dissolution.*
ϕ_6 = *porosity increase due to microfractures.*
a_1 = intergranular pore surface area ratio
a = total surface area ratio
p = laboratory-measured porosity
V_c = total volume of cement
R_p = compaction reduction rate
R_c = *cementation reduction rate.*
R_1 = *dissolution rate.*
a_3 = *microfracture pore surface area ratio.*
R_2 = *the micro-fracture porosity increment rate.*

Data availability

All data generated or analyzed during this study are included in this published article.

References

1. Jia Chengzao, Z. & Min, Z. Unconventional hydrocarbon resources in China and the prospect of exploration and development [J]. *Pet. Explor. Dev.* **39** (2), 129–136 (2012).
2. Zou Caineng, T. et al. New advance in unconventional petroleum exploration and research in China [J]. *Bull. Mineralogy Petrol. Geochem.* **31** (4), 312–322 (2012).
3. Zou Caineng, Z. et al. Geological concepts, characteristics, resource potential and key techniques of unconventional hydrocarbon: on unconventional petroleum geology [J]. *Pet. Explor. Dev.* **40** (4), 385–399 (2013).
4. Zhen, Q. Zou caineng. Unconventional petroleum sedimentology: connotation and prospect [J]. *Acta Sedimentol. Sin.* **38** (1), 1–29 (2020).
5. Zhu Xiaomin, P. et al. Research progress and core issues in tight reservoir exploration. *Earth Sci. Front.* **25** (2), 141–146 (2018).
6. Zhu Xun, F. & Linjie, L. Le, et al. Diagenetic facies and pore evolution of tight sandstone reservoir: taking Sha$_2$ ^{1} *sub-member in the north of Central Sichuan Basin as an example [J]* 29265–270 (Fault-Block Oil & Gas Field, 2022). 2.
7. Zhu Haihua, Z. et al. Alkaline diagenesis and its effects on reservoir porosity: A case study of upper triassic Chang 7 tight sandstones in Ordos basin, NW China [J]. *Pet. Explor. Dev.* **42** (1), 51–59 (2015).
8. Lin Liangbiao, Y. et al. *Reservoir Tightening Process and its Coupling Relationship with Hydrocarbon Accumulation in the Fourth Member of Upper Triassic Xujiahe Formation in the Western Sichuan Depression, Sichuan Basin [J]* 42816–828 (Oil & Gas Geology, 2021). 4.
9. Gao, X. et al. Characteristics of tight sandstone reservoirs and controls of reservoir quality: A case study of the 8 sandstones in the Linxing area, Eastern Ordos basin, China [J]. *Acta Geologica Sinica - Engl. Ed.* **93** (3), 637–659 (2019).
10. Gao, Y. et al. Diagenetic characteristics and quantitative evolution of porosity in tight gas sandstone reservoirs: A case study from the middle and lower permian in the Northwestern Ordos basin. *China [J] Interpretation.* **8** (1), T195–T215 (2020).
11. Jingli, Y. et al. Characteristics of tight oil in triassic Yanchang formation, Ordos basin [J]. *Pet. Explor. Dev.* **40** (2), 150–158 (2013).
12. Chen, Y. et al. Diagenetic facies — a new approach to the prediction of reservoir rocks [J]. *Experimental Petroleum Geol.* **16** (3), 274–281 (1994).
13. Caineng, Z. et al. Concepts, characteristics, potential and technology of unconventional hydrocarbons: on unconventional petroleum geology[J]. *Pet. Explor. Dev.* **40** (4), 413–428 (2013).
14. Li, Z. et al. Logging identification for diagenetic facies of tight sandstone reservoirs: A case study in the lower jurassic Ahe formation, Kuqa depression of Tarim basin [J]. *Mar. Pet. Geol.* **139**, 105601 (2022).
15. Liu, Y. et al. Diagenetic constraints on the heterogeneity of tight sandstone reservoirs: A case study on the upper triassic Xujiahe formation in the Sichuan basin, Southwest China [J]. *Mar. Pet. Geol.* **92**, 650–669 (2018).
16. Li, S. et al. Quantitative characterization of diagenetic reservoir facies of the Karamay alluvial fan in the Junggar basin, Western China [J]. *J. Petrol. Sci. Eng.* **188**, 106921 (2020).
17. Yuan, C. et al. Sedimentological and diagenetic facies of tight sandstones in lacustrine delta-front: A case study of the jurassic Lianggaoshan formation, Eastern Sichuan basin [J]. *Front. Earth Sci.* **12**, 1441548 (2024).
18. Packham, G. H. & Crook, K. A. W. The principle of diagenetic facies and some of its implications[J]. *J. Geol.* **68** (4), 392–407 (1960).
19. Yang Hua et al. Liu Xian yang, Zhang Cai li,. The main controlling factors and distribution of low permeability lithologic reservoirs of Triassic Yanchang For mation in Ordos Basin [J]. *Lithologic Reservoirs*, 19(3): 1–6. (2007).
20. Zheng Rongcai, G. et al. Diagenesis and diagenetic facies of Chang 6 sandstone of Yanchang formation in Baibao area, Ordos basin [J]. *Lithologic Reservoirs*, 19(2): 1–8. (2007).
21. Wang Ruifei, W. & Lixin, L. Diagenesis and porosity evolution of ultra-low permeability and shallow layers sandstone reservoir [J]. *Progress Geophys.* **35** (4), 1465–1470 (2020).
22. Ran Qingchang, Z. et al. Diagenetic facies and porosity evolution of tight sandstone in Shahezi formation [J]. *J. Southwest. Petroleum University(Science Technol. Edition).* **44** (1), 13–26 (2022).
23. Salman Bloch, Lander, R. H. & Bonnell, L. Anomalously high porosity and permeability in deeply buried sandstone reservoirs: origin and predictability [J]. *AAPG Bull.* **86**, 301–328 (2002).
24. Ge JiaWang, Z. et al. A quantitative porosity evolution model of sandstone for Wenchang formation in Huizhou depression, Pearl river mouth basin: A case study for braided fluvial delta reservoir of HZ-A area [J]. *Acta Sedimentol. Sin.* **33** (1), 183–193 (2015).
25. Cao et al. Liu Guang-di, Liu Zhuang-xiao-xue,. Research Status on Tight Oil and Its Prospects [J]. *Natural Gas Geoscience*, **25**(10), 1499–1508 (2014).
26. Wu Hao, J. et al. *Origin of the Paleogene Deep Burial high-quality Reservoirs in the Southern Nanpu Sag [J]* 48553–569 (Journal of China University of Mining & Technology, 2019). 3.
27. Li, Z. et al. Characteristics of fluid inclusion and charging events of natural gas in permian Jiamuhe formation of Zhongguai area, Junggar basin [J]. *Nat. Gas Geoscience.* **24** (5), 931–939 (2013).
28. Wang Xiaoming, C. et al. Diagenetic characteristics and controlling factors of the permian tight sandstone reservoirs in area [J]. *Mar. Geol. Front.* **31** (9), 46–54 (2015).
29. Heyuan, W. et al. An analysis of the zeolite cement in sand-conglomerate and the diagenetic mechanism of Jiamuhe formation, Zhongguai area, Junggar basin [J]. *Acta Petrologica Et Mineral.* **37** (1), 75–86 (2018).
30. Li Zhenhua, Q. et al. Diagenesis of zeolite minerals and its significance for hydrocarbon accumulation in the second member of Jiamuhe formation of Zhongguai area, Junggar basin [J]. *J. China Univ. Petroleum(Edition Nat. Science).* **38** (1), 1–7 (2014).
31. Chen Xinfa, J., Jun, Y. & Haibo Geological characteristics of gas reservoirs in the upper permian Jiamuhe formation in Zhongguai salient, Junggar basin [J]. *Nat. Gas. Ind.* **30** (9), 138–140 (2010).
32. He Wenjun, Y. et al. Comprehensive analysis of tight sandstone gas resource potential in the favorable area of Jiamuhe formation in Xinguang area, Junggar basin [J]. *Nat. Gas Geoscience.* **29** (3), 370–381 (2018).
33. Wang Yaning, Z. et al. Sedimentary facies of triassic in Hong-Che area in Junggar basin [J]. *Xinjiang Petroleum Geol.* **30** (1), 68–72 (2009).
34. Zhang Congzhen, Z. et al. Analysis of sedimentary facies of middle member of permian Jiamuhe formation in Xiaoguai oilfield of Junggar basin [J]. *Xinjiang Petroleum Geol.* **33** (4), 417–419 (2012).
35. Cunhui, F. et al. Development characteristic of reservoir fractures in Jiamuhe formation of Xiaoguai oilfield [J]. *Geol. Sci. Technol. Inform.* **31** (4), 17–21 (2012).
36. Zhang Hongmei, W., Yanjie, D. & Lin Development practice of fracture oilfield with extra-low permeability in Junggar Basin-an example from Xiaoguiai Oilfield[J]. *Xinjiang Petroleum Geol.*, (2): 69–72. (1999).
37. Li Erting, J. et al. *Geochemical Characteristics and Genesis of mid-to-shallow Natural Gas on the Periphery of Shawan Sag, Junggar Basin [J]* 43175–185 (Oil & Gas Geology, 2022). 1.

38. He, X. *Wu Jian-xue, Li Shu-xin, Et Al. Exploration Prospect of Northern Slope in Southern Margin of Junggar Basin [J]*127–129 (Oil Geophysical Prospecting, 2007). S1.
39. Lei Zhenyu, L. et al. *Tectonic Evolution and Development and Distribution of Fans on Northwestern Edge of Junggar Basin [J]*86–91 (Oil & Gas Geology, 2005). 1.
40. Han Bao, W. et al. Controls of the permian unconformity on reservoir formation in Zhongguai-Distriet 5 area of Junggar basin [J]. *Nat. Gas Geoscience*. **28** (12), 1821–1828 (2017).
41. Zhang Zhongpei, Z. et al. *Main Controlling Factors and Exploration Direction of Permian To Triassic Reservior in the Central Sag of Junggar Basin [J]*44559–568 (Petroleum Geology & Experiment, 2022). 4.
42. Wang Jialin, W. et al. Tectonic-depositional environment and prototype basin evolution of the Permian-Triassic in Southern Junggar basin [J]. *J. Palaeogeography*. **18** (4), 643–660 (2016).
43. Li, R. *Characteristics and Classification of Permian Reservoirs in Northwestern Margin of Junggar Basin[J]*78–81 (Oil & Gas Geology, 2001). 1.
44. Caineng Zou, S. et al. Global importance of continuous petroleum reservoirs: accumulation, distribution and evaluation [J]. *Pet. Explor. Dev.* **36** (6), 669–682 (2009).
45. Zhao Yuguang. Sedimentary lithofacies model of permian vocanic-sedimentary basin in Northwestern margin of Junggar basin[J]. *Xinjiang Petroleum Geol.*, (5): 396–400. (1999).
46. Yao, Z. et al. Provenance, depositional environment, and paleoclimatic conditions of a Near-Source fan delta: A case study of the permian Jiamuhe formation in the Shawan sag, Junggar basin. *Minerals* **13** (10), 1251 (2023).
47. Hui, X. et al. *Influence of Diagenetic Evolution on Tight Sandstone Reservoir Flow Capacity: Chang 8 Reservoir of Yanchang Formation in Southern Maling, Ordos Basin [J]*41800–811 (Petroleum Geology & Experiment, 2019). 6.
48. Lan, Y. F., Huang, S. J. & Lü, J. Influences of authigenic chlorite on pore structure in sandstone reservoir: A case study from upper triassic Yanchang formation in Ordos basin, China [J]. *Geol. Bull. China 2011*, **30**(1): 134–140 .
49. Peters, K. E. & Moldowan, J. M. *The Biomarker Guide: Interpreting Molecular Fossils in Petroleum and Ancient Sediments [J]* (Englewood Cliffs Nj Prentice Hall, 1993).
50. Przyjalgowsky, M. A. et al. *Analysis of hydrocarbon-bearing Fluid Inclusions (HCFI) Using time-resolved Fluorescence Spectroscopy [C]//Opto-ireland* (Optical Sensing & Spectroscopy, 2005).
51. Pan Xuefeng. *Research and application on reservoir fluid inclusion technology [D]*. Southwest Petroleum University Doctoral Dissertation, (2013).
52. Beard, D. C. & Wely, P. K. Influence of texture on porosity and permeability of unconsolidated sand [J]. *AAPG Bull.* **57** (2), 349–369 (1973).
53. Scherer, M. Parameters influencing porosity in sandstones: A model for sandstone porosity prediction: Erratum[J]. *AAPG Bull.*, 71. (1987).
54. Zou Caineng, T. et al. Genesis classification and evaluation method of diagenetic facies [J]. *Pet. Explor. Dev.*, (5): 526–540. (2008).
55. Chen Xianliang, J. & Youliang, Y. K. *Diagenetic Facies Distribution Within the Upper Shaximiao Formation Sequence Framework in the Middle Part of Western Sichuan [J]*23173–176 (Special Oil & Gas Reservoirs, 2016). 6.

Acknowledgements

Author contributions

Yao Zongquan and Fu Tianyu wrote the mian manuscript text Wang Jun and Wang Wei prepared visualizationZhang Xiaohong conducted a validation study to assess the reliability of the resultsJia Chunming, Yu Haitao, and Li Jing are in charge of project administrationDeleqiati` Jianatayi and Wang Haoyi conducted a format analysis and survey.

Declarations

Competing interests

The authors declare no competing interests.

Additional information

Correspondence and requests for materials should be addressed to Y.Z.

Reprints and permissions information is available at www.nature.com/reprints.

Publisher's note Springer Nature remains neutral with regard to jurisdictional claims in published maps and institutional affiliations.